

# Evaluation of Velocity Estimation Methods Based on their Effect on Haptic Device Performance

Vinay Chawda, *Member, IEEE*, Ozkan Celik, *Member, IEEE*  
and Marcia K. O'Malley, *Senior Member, IEEE*

**Abstract**—This paper comparatively evaluates the effect of real-time velocity estimation methods on passivity and fidelity of virtual walls implemented using haptic interfaces. Impedance width, or Z-width is a fundamental measure of performance in haptic devices. Limited accuracy of velocity estimates from position encoder data is an impediment in improving the Z-width in haptic interfaces. We study the efficacy of Levant's differentiator as a velocity estimator, to allow passive implementation of higher stiffness virtual walls as compared to some of the commonly used velocity estimators in the field of haptics. We first experimentally demonstrate feasibility of Levant's differentiator as a velocity estimator for haptics applications by comparing Z-width performance achieved with Levant's differentiator and commonly used Finite Difference Method (FDM) cascaded with a lowpass filter. A novel Z-width plotting technique combining passivity and fidelity of haptic rendering is proposed, and used to compare the haptic device performance obtained with Levant's differentiator, FDM+lowpass filter, First Order Adaptive Windowing and Kalman filter based velocity estimation methods. Simulations and experiments conducted on a custom single degree of freedom haptic device demonstrate that the stiffest virtual walls are rendered with velocity estimated using Levant's differentiator, and highest wall rendering fidelity is achieved by First Order Adaptive Windowing based velocity estimation scheme.

## I. INTRODUCTION

Impedance width, or Z-width is defined as the dynamic range of achievable impedances that can be rendered by a haptic interface device, where *achievable impedances* mean that impedances satisfy a robustness property, such as passivity [1]. The upper limit of Z-width is the *maximum impedance* that can be rendered by a haptic interface without any voluntary human motion induced instabilities [2]. Z-width is a fundamental measure of performance in haptic interfaces, and a higher Z-width means that a wide range of haptic environments can be rendered by the device. Z-width is an important metric to compare performance of haptic devices used for rendering complex virtual environments for surgical applications [3]. The haptic device must be able to render impedances that occur in such virtual environment interactions in a stable manner. Need for maximal Z-width performance has also been recognized as one of the essential requirements in haptic tele-manipulation of surgical robots [4]. Various strategies have been proposed to increase the Z-width of haptic interfaces, such as increasing the sampling frequency [5], increasing encoder resolution, adding physical damping [1], adding electrical damping [6], [7] and hybrid control algorithms that employ both active and passive actuators (such as magneto-rheological brakes) [8], [9]. Few researchers, however, have investigated the effect of velocity estimation accuracy on the Z-width performance. In one case, Hayward et al. proposed an Adaptive Windowing discrete-time velocity estimation technique and presented as an example its

application to improve Z-width performance [10]. In other work, Gil explored the effect of FDM+filter parameters on the Z-width performance in simulation [11]. Colonnese and Okamura [12] presented explicit stability and quantization error regions for virtual spring and damper rendering, offered a software tool to identify system parameters necessary to satisfy desired haptic display objectives, and verified their findings experimentally. In [13], we proposed use of the Levant's differentiator for estimating velocity, and presented preliminary results on Z-width improvement.

Finite Difference Method (FDM) is the most widespread method used for estimating velocity from position encoder data in haptic applications. As the sampling rates increase, the velocity resolution deteriorates significantly for FDM [14]. Cascading FDM with a lowpass filter is a common way of addressing the issue of poor velocity resolution at high sampling rates [1], but this comes at the cost of introducing a time-delay in velocity estimation. Time-delay in velocity estimation acts as another limiting factor in increasing the Z-width of haptic displays. There is a trade-off between the noise admitted and the time-delay in estimation: lower the cutoff frequency, less the noise admitted into the system, but with greater time-delay in estimations, and vice versa. This trade-off has been widely explored in the literature [15] and various velocity estimation schemes have been proposed to overcome the limitations of FDM+filter with varying degrees of success, such as adaptive windowing [16], time stamping [17], Kalman filter based [14], curve breaking velocity estimator [18] and Least Squares fit based [19] techniques. Tilli and Montanari discussed the shortcomings of FDM+filtering and other differentiation techniques, and proposed a switching filter approach for velocity estimations from discrete position readings in [20]. In [21], Koul et al. proposed a dual-rate sampling scheme that decouples the position and velocity control loops, and employs a slower sampling rate for velocity control loop to reduce the quantization effects in FDM based velocity estimation to improve the Z-width performance. Sinclair et al. [22] presented a comparative experimental evaluation of a variety of velocity estimation algorithms including several hybrid combinations of more than one algorithm.

Velocity estimation techniques from position encoder signal can be broadly divided into two categories: period counting and frequency counting methods. Period counting methods use specialized hardware to accurately measure the time elapsed between consecutive encoder ticks, and use that to estimate velocity [23], [24], [25]. A primary advantage of period counting methods is in very accurate estimation at low velocities, but the resolution degrades at higher velocities. Frequency counting methods use number of encoder ticks per unit time information to estimate the velocity. Zhu and Lamarche proposed a velocity estimation technique using both position and acceleration data, for damping enhancement in haptic devices [26]. Again, the drawback

is the need for additional hardware. To circumvent differentiation induced effects, in [27] and [28] authors propose using fractional order control that employs differentiation and integration of arbitrary order. Controller designed using this approach is shown to enlarge the Z-width as compared to standard integer order differentiation based control. While this approach provides an additional degree of freedom in increasing Z-width, limitations exist due to sensitivity to changes in system parameters and distortion of effective inertia at higher frequencies. A good derivative estimation scheme should exhibit zero or minimum time-delay in estimations, provide increasing accuracy with increasing sampling frequency, robustness to fluctuations in input signal velocity, and offer ease of implementation on existing hardware. To that end, in our previous work [13], we proposed the use of the Levant's differentiator for improved velocity estimations and increased Z-width in haptic interfaces.

Levant's differentiator is a Second Order Sliding Mode (SOSM) control based real-time robust exact differentiation technique [29]. It is a nonlinear velocity observer which exhibits finite time convergence and increasing accuracy with increasing sampling rates. In [13] we performed a preliminary feasibility study of the Levant's differentiator as a velocity estimator for haptic interfaces, and compared it with the FDM+filter method. Convergence of Levant's differentiator is contingent upon the choice of several parameters, and a crude condition for choosing them was given by Levant in [29].

In this paper, we use the Lyapunov function analysis technique for SOSM systems proposed in [30] to extend the range of acceptable choice of parameters that would ensure convergence of Levant's differentiator. Levant's differentiator implementations with parameters chosen according to Levant's recommendations, Lyapunov analysis and from experimental tuning are compared with FDM+lowpass filter method in their effectiveness in increasing Z-width performance of a custom one degree of freedom haptic device. We additionally propose a novel format for Z-width plots, which present virtual wall stiffness (K) vs. virtual wall damping (B). A detailed review of performance metrics for haptic interfaces by Samur in [2] presents the frequency domain max/min impedance range plotting method proposed by Weir et al. [7] as the state of art for quantifying the Z-width. However, frequency domain plots still do not provide information on accuracy of the rendered impedance. An improved plot was proposed by Baser et al. [8] where Z-Width is presented together with transparency bandwidth. In [31], Gil et al. presented a method of estimating Z-width using the experimental frequency response computed at different workspace positions, and critical stiffness values are then plotted as isolines in the workspace. This method extends the traditional Z-width plot by showing the dependence on workspace position, however does not inform about fidelity of the achievable impedances. Our plotting method simultaneously illustrates the stable K-B region and the fidelity of the rendering at each stable K-B pair, overcoming limitations with the traditional time-response based method of plotting Z-width that fails to capture the device inertia, mechanical resonances, and fidelity of the rendered virtual environment, and provides a more comprehensive fidelity measure. Our fidelity of rendering measure builds upon the frequency response-based Z-width plotting method proposed in [7]. Colonnese et al. define the Average Distortion Error (ADE) as a metric for describing haptic accuracy and form an objective function to optimally

compute linear system model parameters in [32]. ADE quantifies frequency dependent difference between actual and desired dynamics, normalized by desired dynamics and multiplied by a weighting function. The fidelity measure employed in this paper can be thought of as a simplified ADE without normalization and a unity weighting function. This combined Z-width plot captures the practical limitations of haptic devices which are not evident in time-response based Z-width computation, and also provides information about fidelity of the commanded virtual environment. The idea is simple but effectively conveys the information about both stability and accuracy in an easily recognizable format. Our proposed Z-width plotting method is employed to compare the Levant's differentiator with FDM+lowpass filter, First Order Adaptive Windowing (FOAW) and Kalman filter based methods in both simulations and experiments. Results show that among all the velocity estimation schemes considered, highest stiffness virtual walls are rendered with Levant's differentiator, while First Order Adaptive Windowing enabled rendering virtual walls with highest fidelity.

## II. REVIEW OF VELOCITY ESTIMATION METHODS

In this section we briefly review the velocity estimation methods considered in this paper. These methods are chosen based on their widespread use for estimating velocity in haptics applications.

### A. FDM+lowpass filter

Finite Difference Method (FDM) is the most basic method of estimating velocity by computing the slope of two most recently sampled position data points, given as:

$$v_k = \frac{y_k - y_{k-1}}{T} \quad (1)$$

where  $y_k$  is the discrete position signal obtained by sampling the continuous position signal  $y(t)$  at  $t = kT$  time instants, where  $T$  is the sampling period.  $v_k$  is the estimated velocity. However, high sampling rates ( $\geq 1$  kHz) typically used in haptic applications will significantly amplify any noise present in  $y_k$  [16]. The most commonly used method for removing high frequency noise in velocity estimations induced by FDM is implementing a low-pass filter. In our study, we used a second order Butterworth filter to remove the noise in FDM-based velocity estimations, which is a well-known and commonly used filter in haptic and other feedback control systems. The tunable parameter in FDM+filter method is the filter cutoff frequency  $\omega_c$ , which can be tuned to achieve best performance. We selected the filter cutoff frequency  $\omega_c$  to maximize the Z-width performance as detailed in [15].

### B. Kalman filter

Kalman filtering of the measured position signal based on a triple-integrator model to estimate velocity was proposed by Bélanger in [14]. Although a double-integrator model will suffice for estimating velocity, Bélanger recommends using a triple integrator model for increased accuracy. Using the notation in [16], a linear discrete stochastic model is used to represent the estimated state  $\mathbf{x}_k$  as:

$$\mathbf{x}_{k+1} = \mathbf{A}\mathbf{x}_k + \mathbf{G}\mathbf{w}_k \quad (2)$$

$$y_k = \mathbf{H}\mathbf{x}_k + e_k \quad (3)$$

where  $\mathbf{x}_k = (x_k, \dot{x}_k, \ddot{x}_k)$  is a vector of the estimated position  $x_k$  and its derivatives,  $A$  is the state transition matrix,  $H$  is the observation matrix and  $y_k$  is the position measured at  $k^{th}$  sampling instants.  $\mathbf{w}_k$  is the process noise and  $e_k$  is the measurement noise, both of which are assumed to be zero mean white Gaussian. Since we have assumed the triple-integrator model,  $A$ ,  $G$  and  $H$  are given as:

$$A = \begin{bmatrix} 1 & T & \frac{T^2}{2} \\ 0 & 1 & T \\ 0 & 0 & 1 \end{bmatrix}, G = \begin{bmatrix} 1 & 0 & 0 \\ 0 & 1 & 0 \\ 0 & 0 & 1 \end{bmatrix}, H = [1 \ 0 \ 0]. \quad (4)$$

In the triple-integrator model,  $\mathbf{w}_k$  is viewed as a surrogate for derivative of acceleration, and therefore its covariance matrix  $Q_k$  can be written as

$$Q_k(i, j) = \frac{q}{(3-i)!(3-j)!(7-i-j)!} T^{7-i-j}$$

where  $q$  is a parameter that needs to be adjusted depending on the motion characteristics. We tuned the parameter  $q$  in simulation to maximize the impedance width performance. Typically, in commercially available haptic devices, position is sensed from an optical position encoder, where error in measurement is predominantly due to quantization, such that  $-d \leq e_k \leq d$  where  $d$  is the encoder resolution. Thus, variance for the measurement error  $e_k$  is given as  $r = \text{var}(e_k) = d^2/3$ . Based on the above model, an Adaptive fading Kalman Filter can be written to estimate velocity as detailed in [16] and [33].

### C. Adaptive windowing

Janabi-Sharifi et al. proposed a discrete-time First Order Adaptive Windowing (FOAW) method which addresses the noise amplification issue present in FDM by adaptively changing the window size for computing the velocity based on the signal itself [16]. This is equivalent to adaptively changing the sampling rate. Window size is chosen short when the velocity is high, and large when velocity is low; thereby providing more precise and reliable velocity estimates. The goal is to find a straight line that passes through the sampled data  $y_k, y_{k-n}$  over a window of length  $n$  where  $n = \max\{1, 2, 3, \dots\}$  such that

$$|y_{k-i} - y_{k-i}^f| \leq d, \quad \forall i \in \{1, 2, \dots, n\} \quad (5)$$

where  $y_{k-i}^f = a_n + b_n(k-i)T$ . For Best-fit-FOAW solution, the coefficients  $a_n$  and  $b_n$  are given as:

$$\begin{aligned} a_n &= \frac{ky_{k-n} + (n-k)y_k}{n} \\ b_n &= \frac{n \sum_{i=0}^n y_{k-i} - 2 \sum_{i=0}^n i y_{k-i}}{Tn(n+1)(n+2)/6}. \end{aligned} \quad (6)$$

Here  $b_n$  is the slope of the best-fit line computed using least-square approximation which minimizes the error energy. The estimated velocity is  $\hat{v}_k = b_n$ . The algorithm for FOAW is given in [16].

## III. LEVANT'S DIFFERENTIATOR FOR VELOCITY ESTIMATION

Levant proposed a robust exact differentiation technique using SOSM for signals with a given upper bound on the Lipschitz's constant of the derivative [29]. Given an input signal  $f(t)$ , the Lipschitz's constant of the derivative is a constant  $C$  which satisfies

$$|\dot{f}(t_1) - \dot{f}(t_2)| \leq C|t_1 - t_2| \quad (7)$$

If the second derivative of the base signal exists, then the Lipschitz's constant in (7) satisfies

$$\sup_{t \geq 0} \left| \frac{d^2}{dt^2} f(t) \right| \leq C \quad (8)$$

Consider  $x(t)$  an estimate of the input signal  $f(t)$ . Define error in the estimate as  $e(t) = x(t) - f(t)$ , then the first order derivative can be estimated as

$$\begin{aligned} \dot{x}(t) &= u(t) \\ u(t) &= u_1(t) - \lambda|e(t)|^{1/2} \text{sign}(e(t)) \\ \dot{u}_1(t) &= -\alpha \text{sign}(e(t)) \end{aligned} \quad (9)$$

The solution of the system described by equation (9) is understood in the sense of Filippov [34].  $\lambda$  and  $\alpha$  are strictly positive constants which determine the differentiation accuracy and must be chosen properly to ensure convergence. Levant proposed a homogeneity based approach (HBA) for proving the convergence of the SOSM based differentiator and recommended conditions on the gains  $\lambda$  and  $\alpha$  such that the differentiator is stable. We present a Lyapunov function based approach (LFBA) to extend the stability conditions given by HBA. Both stability criteria are discussed in the following subsections.

### A. Levant's stability criteria

Levant proposed a sufficient condition [29] for finite time convergence of  $u(t)$  to  $\dot{f}(t)$ , given as

$$\alpha > C, \quad \lambda^2 \geq 4C \frac{\alpha + C}{\alpha - C} \quad (10)$$

An easier choice of the parameters given in the same reference is

$$\alpha = 1.1C, \quad \lambda = C^{1/2} \quad (11)$$

It should be noted that conditions (10) and (11) result from a very crude estimation of the convergence criterion.

### B. Lyapunov function based stability criteria

Using the Lyapunov function analysis for the second order sliding mode systems proposed in [30], we can extend the stability conditions proposed by Levant in (10) to increase the range of acceptable values of parameters  $\alpha$  and  $\lambda$ .

Using the reformulation proposed in [30], the system (9) can be re-written as follows:

$$\begin{aligned} \dot{x}_1(t) &= -\lambda|x_1(t)|^{1/2} \text{sign}(x_1(t)) + x_2(t) \\ \dot{x}_2(t) &= -\alpha \text{sign}(x_1(t)) - \dot{f}(t) \end{aligned} \quad (12)$$

where  $x_1(t) = e(t) = x(t) - f(t)$  and  $x_2(t) = u_1(t) - \dot{f}(t)$ . We consider a Lyapunov function candidate given as:

$$\begin{aligned} V(x) &= 2\alpha|x_1| + \frac{1}{2}x_2^2 + \frac{1}{2}(\lambda|x_1|^{1/2} \text{sign}(x_1) - x_2)^2 \\ &= \zeta^T P \zeta \end{aligned} \quad (13)$$

where  $\zeta = [|x_1|^{1/2} \text{sign}(x_1) \quad x_2]^T$  and

$$P = \frac{1}{2} \begin{bmatrix} 4\alpha + \lambda^2 & -\lambda \\ -\lambda & 2 \end{bmatrix}$$

Using the Lyapunov function candidate detailed above and following the analysis detailed in [30], the stability conditions

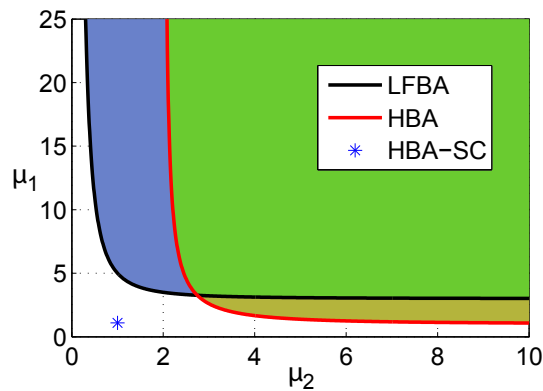


Fig. 1. The shaded regions show stable pairs of gains  $(\alpha, \lambda)$  based upon the Lyapunov Function Based Approach (LFBA) and the Homogeneity Based Approach (HBA). The HBA-SC is the special case gain pair proposed by Levant [29].

derived from the Lyapunov Function Based Approach (LFBA) are given as:

$$\alpha > 3C + \frac{2C^2}{\lambda^2}; \lambda > 0 \quad (14)$$

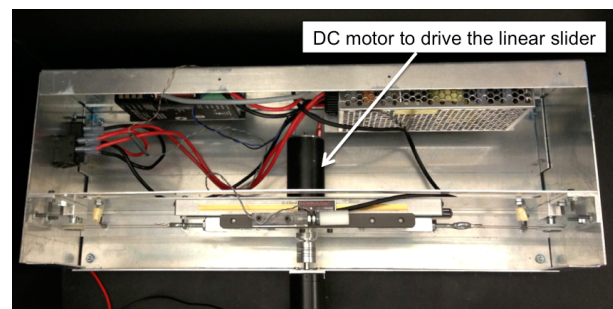
The stability conditions obtained from the HBA and LFBA can be compared by using the parameterization  $\alpha = \mu_1 C$  and  $\lambda = \mu_2 C^{1/2}$ , to eliminate the Lipschitz's constant  $C$  from the inequalities. The plots of  $\mu_1$  vs.  $\mu_2$  give the parameterized stable regions as shown in Fig. 1. It can be observed that LFBA stability conditions, while not wholly encompassing the HBA conditions, do extend the range of choice for the parameters  $\alpha$  and  $\lambda$ . It is observed that the HBA-Special Case (HBA-SC) gain pair given by (11) lies outside of the both regions. Since both LFBA and HBA give only sufficient conditions, it is possible to choose a gain pair which lies outside these stability ranges but still ensures convergence. For this study, the gains were chosen to satisfy the stability conditions and maximize Z-width performance in simulation.

#### IV. FEASIBILITY OF LEVANT'S DIFFERENTIATOR FOR INCREASING Z-WIDTH

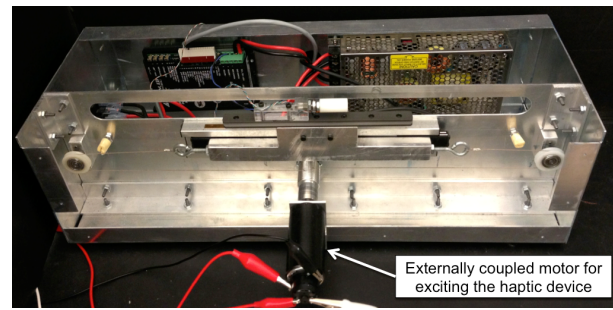
In this section, we investigate the feasibility of Levant's differentiator as a velocity estimator in increasing the Z-width performance in haptic interfaces. We followed the automated Z-width estimation experimental protocol described in [13] to estimate the Z-width of a custom linear impedance type haptic device shown in Fig. 2. Control of the haptic device was implemented in Simulink<sup>®</sup> and QuaRC<sup>®</sup> on a host computer running Windows<sup>®</sup>. The code is compiled and downloaded on a target computer running QNX<sup>®</sup> RTOS, which is interfaced to the haptic device through a Q4 DAQ from Quanser Inc. The sampling rate was set at 10 kHz.

A spring-damper virtual wall was implemented and Z-width was computed using time-response data collected during virtual wall hit trials. The virtual wall stiffness ( $K$ ) and virtual wall damping ( $B$ ) values were varied and the pairs of  $(K, B)$  which presented a marginally passive virtual wall interaction are recorded. For evaluating the feasibility of Levant's differentiator, the Z-width plot is computed for the following velocity estimation methods:

- 1) Levant's differentiator with the HBA-SC gains.
- 2) Levant's differentiator with the LFBA gains.



(a) Top view



(b) Front view

Fig. 2. The single degree-of-freedom haptic device used for Z-width estimation.

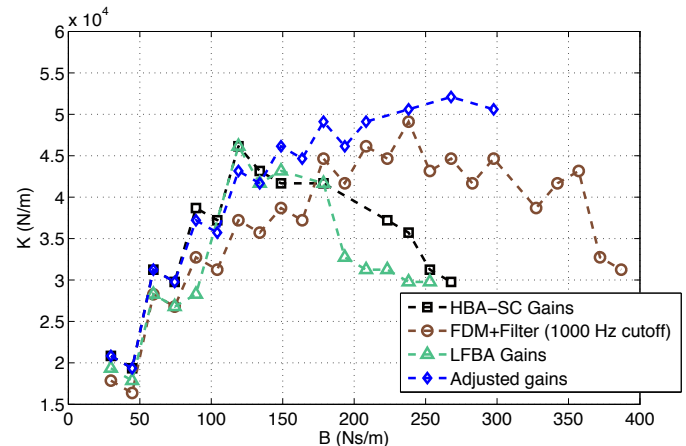


Fig. 3. Experimental time-domain Z-width estimation with various differentiation schemes during automated wall-hitting trials.

- 3) Levant's differentiator with experimentally adjusted gains.
- 4) FDM cascaded with a second order Butterworth filter with 1000 Hz cutoff frequency.

The value of Lipschitz's constant is calculated by collecting the position data during a virtual wall hit with velocity estimated using FDM cascaded with a second order Butterworth filter, and calculating the analytical double derivative of a sum of sines function fitted to the position data. The cutoff frequency for the Butterworth filter was chosen experimentally to get the maximum Z-width performance.

It is observed in Fig. 3 that use of Levant's differentiator with adjusted gains for velocity estimation extends the Z-width of the device (higher virtual wall stiffness), as compared to using FDM+filter for the same purpose. Levant's differentiator with HBA and LFBA based gains performs better than FDM+filter for damping values up to 150 Ns/m, but is found to be conservative.

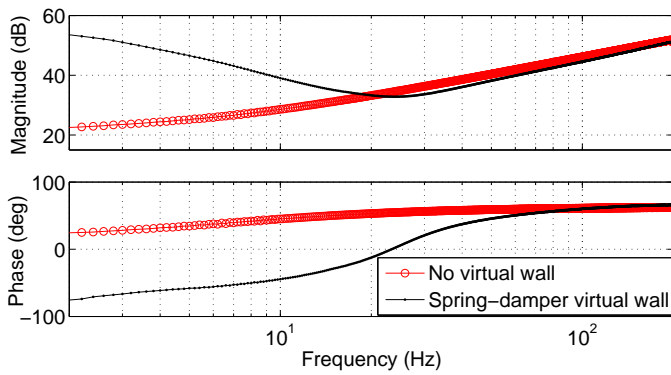


Fig. 4. Impedance transfer function plots obtained in simulation for a single degree of freedom linear haptic device with quantization, sampling and coulomb friction nonlinearities.

We adjusted the gains experimentally, thereby further increasing the Z-width of the device. FDM+filter with a 1000 Hz cutoff allowed stable rendering of walls with higher damping values ( $> 350$  Ns/m) but with lower stiffness than those were possible with Levant’s differentiator at lower damping values. Unlike the Z-width plots for FDM+filter methods, when Levant’s differentiator is used, the stable region ends with a sharp drop at a specific damping value. This value is around 250 Ns/m for Levant’s differentiator with HBA and LFBA gains and it is around 300 Ns/m for Levant’s differentiator with adjusted gains. The reason for this sharp drop is as  $K$  and  $B$  increase, the gains  $\alpha$  and  $\lambda$  selected for the nominal case by estimating  $C$  or the ones found experimentally are no longer proper. This causes significant increase in chatter at the equilibrium position resulting in an unstable hit. A different choice of gains can extend the Z-width to higher  $B$  values but may lose stability in the lower range.

#### V. COMPARISON OF VELOCITY ESTIMATORS

In the previous section we showed the feasibility of Levant’s differentiator as a velocity estimator for increasing Z-width performance in haptic interfaces. However, Z-width was computed based on time-response data recorded during wall-hit trials with varying  $K$  and  $B$  values, where passivity was quantified by absence of sustained or growing oscillations after virtual wall interactions. A more illustrative method for computing and plotting Z-width information was proposed by Weir et al. in [7], where the envelope of passive impedances that can be rendered by a haptic display is plotted. The haptic device impedance is estimated by providing an external multi-sine excitation signal to the device and estimating an impedance transfer function by considering velocity as input and force as output. Fig. 4 shows the impedance plots obtained with no virtual wall and when a virtual wall was being rendered.

This method has the advantage of capturing the practical device characteristics such as device inertia and mechanical resonances which are overlooked in Z-width estimation using time-response data [7]. However, fidelity of the rendered virtual wall is still not captured. We propose a novel Z-width plotting method which combines the higher information density of Z-width computed using frequency-response data with the intuitive nature of  $K$ - $B$  plots based on time-response data. The impedance transfer functions are estimated for  $(K, B)$  pairs in an exhaustive grid-based scheme, and if the phase of the estimated transfer function

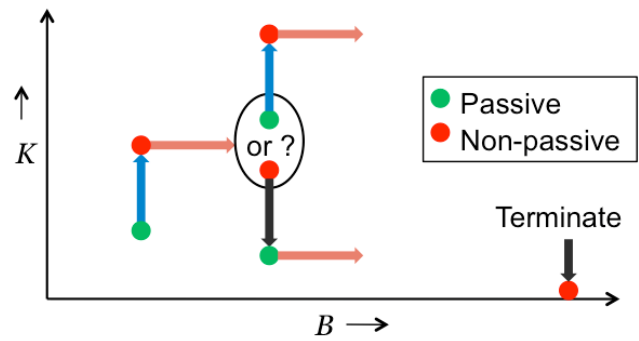


Fig. 5. Grid based search scheme for exploring the virtual wall impedance space  $(K, B)$  and generating the Z-width plots.  $K$  is virtual wall stiffness and  $B$  is virtual wall damping.

is between  $\pm 90$  degrees over the useful range of the device, the virtual wall corresponding to that particular  $(K, B)$  pair is declared passive. Search begins with nominal initial stiffness and damping value pair  $(K, B)$  for which the virtual wall is passive. Passivity of the impedance transfer function for various  $(K, B)$  values is tested by incrementing  $K$  in steps for a particular value of  $B$  until the system is not passive. Then  $B$  is incremented by one step and if the transfer function is still not passive,  $K$  is decremented until a passive transfer function is obtained; and if the transfer function is passive then  $K$  is incremented until it becomes non-passive. Either way, once the passivity boundary is reached,  $B$  is incremented and the cycle is repeated. The search terminates when  $K \rightarrow 0$ . Fig. 5 shows the scheme graphically. Fidelity of the rendered virtual wall is quantified by computing the Root Mean Square (RMS) difference between the magnitude plots of the estimated impedance transfer function and the ideal spring-damper transfer function as shown in Fig. 6. This RMS difference is a measure of how well the rendered wall matches the commanded spring-damper virtual wall. Conventional methods of plotting Z-width only show the range of impedances that satisfy the passivity condition (i.e. phase is between  $\pm 90$  degrees), however this added metric captures the fidelity of a desired impedance when rendered by a haptic interface. Quantifying performance of a haptic interface in rendering a given impedance should involve assessing both the passivity and fidelity of rendered impedance. It can be observed that at low frequencies the magnitude plot of estimated impedance matches the ideal wall impedance quite well, but at higher frequencies the device inertia becomes prominent and the controller can no longer render the commanded virtual wall. The slight attenuation in magnitude of the estimated impedance at low frequencies can be attributed to nonlinearities such as friction, quantization and sampling.

The velocity estimation methods described in Section II are compared in simulations and experiments using our proposed Z-width plotting method. For simulation, the device model parameters were identified by performing frequency domain system identification of the haptic device shown in Fig. 2 using a Schroeder phased input signal [35] and the System Identification Toolbox<sup>©</sup> in Matlab<sup>©</sup>. Static and kinetic friction are assumed to be the same, and was estimated a priori and compensated before performing frequency domain system identification. A mass-damper model with Coulomb friction was assumed, and the estimated parameters were mass  $m = 0.52$  kg, damping  $b = 13.2$  Ns/m and Coulomb friction  $f_c = 0.19$  N. The haptic device

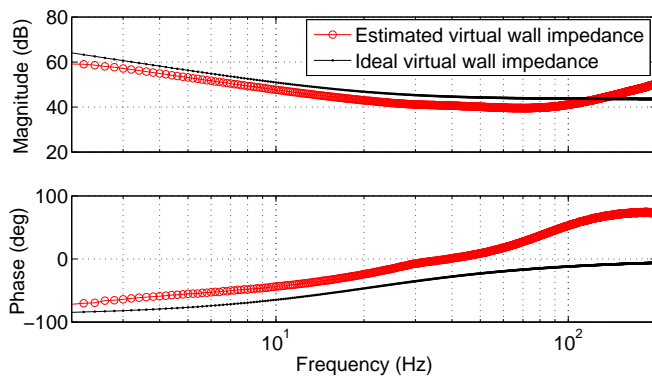


Fig. 6. Estimated impedance of the haptic device compared with the ideal impedance expected from a spring-damper virtual wall. Note that at higher frequencies, device inertia becomes prominent and the deviation from ideal spring-damper virtual wall case increases.

simulation rate was set at 1 kHz and position quantization was  $1\mu\text{m}$ , corresponding to the experimental setup. An external multi-sine perturbation force was applied to excite the device, and the velocity and force signals were sampled at 4 kHz. The *tfestimate* function in Matlab<sup>®</sup> was used to estimate the impedance transfer function of the rendered haptic environment. The Z-width plots obtained with various velocity estimation methods are shown in Fig. 7. The tunable parameters in all velocity estimation methods were chosen to achieve best possible performance, and were selected to be  $\omega_c = 499$  Hz for FDM+filter,  $q = 2.5 \times 10^4$  for the AKF method and  $\alpha = 6.6, \lambda = 2.45$  for the Levant’s differentiator.

Experimental Z-width computation was done by attaching an external motor to the haptic device as shown in Fig. 2 to apply a multi-sine perturbation signal to the haptic device. The haptic environment was rendered at 1 kHz. Velocity and force signals were sampled at 4 kHz for estimating the impedance transfer function. Tunable parameters for all velocity estimation methods were chosen to be same as the simulation. The Z-width plots computed experimentally are shown in Fig. 8.

It can be observed from the simulation and experimental Z-width plots shown in Figs. 7 and 8 that highest virtual wall stiffness is obtained with Levant’s differentiator, then AKF, followed by FDM+filter and FOAW. Several other interesting observations can be made from the Z-width plots. First, in both simulations and experiments, accuracy of the rendered virtual wall is higher for lower values of  $K$  and  $B$ . This is expected because higher values of  $K$  and  $B$  may saturate the actuator over frequency range near resonance, causing significant deviations from the expected ideal wall impedance characteristics. Higher  $B$  amplifies the noise and delay present in velocity estimations, which causes deviations from the ideal wall case before the haptic interaction is ultimately rendered non-passive. Second, the ranges of Z-width plots computed experimentally can be observed to be smaller than the corresponding simulation plots. This can be attributed to mechanical vibration modes and other nonlinearities that were not captured in the simplified linear model assumed in the simulation. Finally, the Z-width plots for Levant’s differentiator and FDM+filter shown in Figs. 8(a) and 8(d) match the trend observed with  $K$ - $B$  plots shown in Fig. 3. In both cases, the Levant’s differentiator was able to achieve a higher stiffness value as compared to FDM+filter, but was limited in displaying higher virtual damping.

Table I compares the experimental Z-width results for various differentiation schemes along following metrics: maximum rendered stiffness (K-width), maximum rendered damping (B-width), maximum fidelity error and number of parameters to be tuned. These metrics are chosen to compare the suitability of differentiation schemes for any given application. It can be seen that Levant’s differentiator is able to achieve highest K-width, but is limited in B-width. Furthermore, Levant’s differentiator requires two parameters to be tuned and displays second highest fidelity error. Both FDM+filter and AKF display intermediate K-widths and require a single parameter to be tuned. FDM+filter is able to achieve highest B-width, but also has highest fidelity error of all schemes. FOAW displays smallest K-width, but requires no parameter tuning and displays smallest fidelity error. None of the schemes perform best across all the metrics, so depending on the application, appropriate scheme (or combination thereof) needs to be selected. For example, if low damping and high stiffness is desired, then Levant’s differentiator is a good choice, but if intermediate damping and stiffness are desired, then FOAW is better. A combination of multiple differentiation schemes, such as FOAW and Levant’s differentiator could potentially result in better performance than each of them individually.

In related work, Sinclair et al. [22] experimentally compared a variety of velocity estimation algorithms. They optimized each algorithm’s relevant parameters using a pure adaptive search method to minimize a multi-objective criterion that took into account both the delay and the error in delay-corrected velocity estimations. Based on this criterion, third order Kalman estimators that were hybrid combinations of the Kalman estimator with Levant’s differentiator or FOAW produced the smallest error in estimations. The focus of the work was realistic haptic simulation of stick-slip sensations, therefore virtual-wall specific evaluations of the estimators were outside the scope of this work. Indeed, Sinclair et al. pointed to the distinctly different aspects of performance that virtual wall and stick-slip haptic simulations require from velocity estimators. The FOAW method did not perform well in comparison with the other algorithms in Sinclair et al.’s work. In our work, however, it has shown the best performance when viewed from the haptic fidelity perspective.

In this paper, we have only considered the SOSM based robust exact differentiation technique proposed by Levant in [29]. Other variations and extensions to this technique have been proposed since then combine the SOSM and Linear observers and/or propose variable gain structure where the parameters  $\alpha$  and  $\lambda$  are updated according to a set of relations [36], [37], [38]. These extensions introduce more parameters which need to be selected and tuned based on simulation or experiments, thus increasing the complexity of the implementation. When properly tuned, these extensions to SOSM based velocity observer may provide better velocity estimates than the standard Levant’s differentiator discussed in this paper.

Successful implementation of Levant’s differentiator for velocity estimation demonstrated increased K-width performance in haptic interfaces as compared to FDM+filter, AKF and FOAW velocity estimation methods in both simulations and experiments. Ease of implementation and finite-time convergence characteristics of the Levant’s differentiator makes it an attractive option for use as a velocity estimator in haptics and other feedback control system applications.

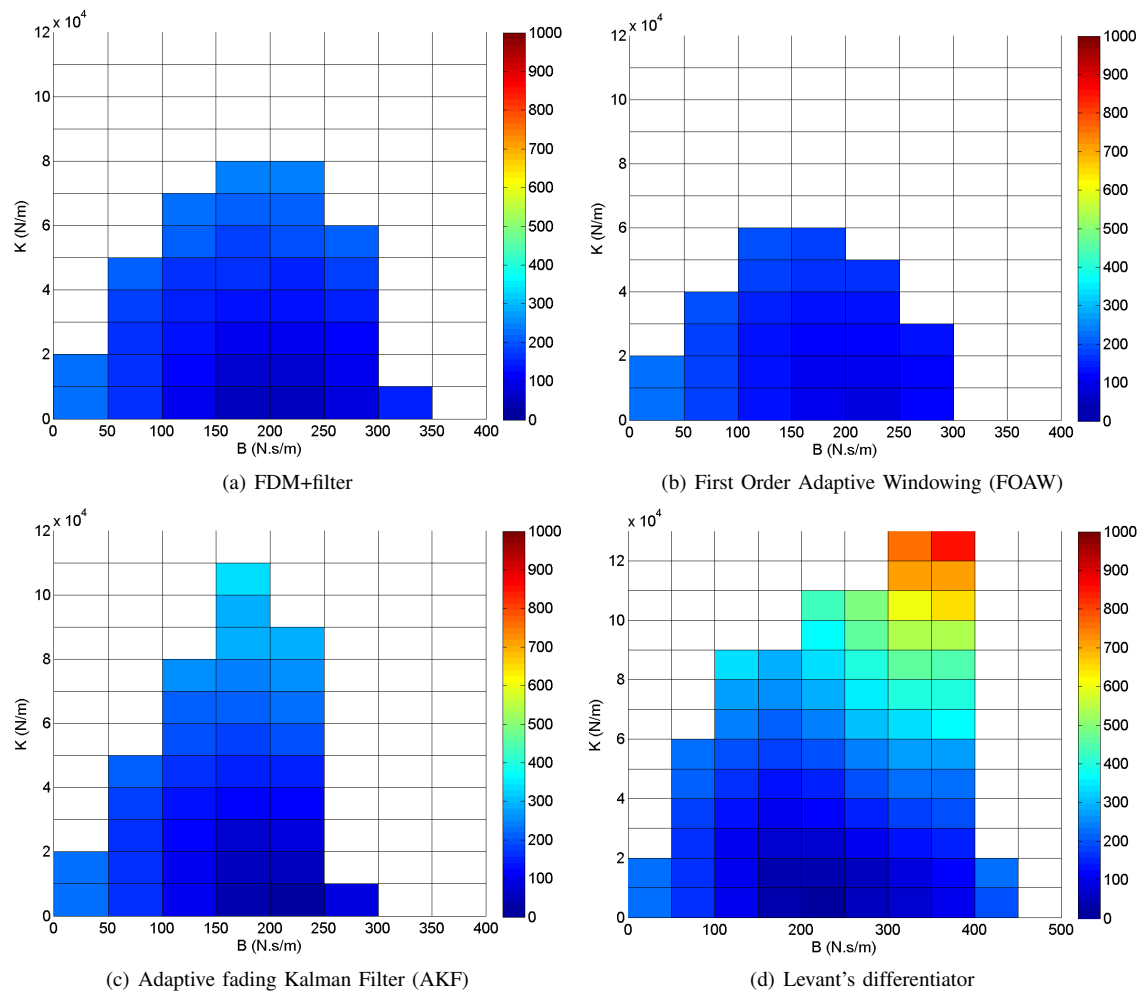


Fig. 7. Z-width plots obtained in simulation for various velocity estimation methods. The colorbar shows the RMS error (in Ns/m) between estimated and ideal virtual wall impedance. It is observed that highest virtual wall stiffness is obtained with Levant's differentiator, then AKF, followed by FDM+filter and FOAW. The fidelity of haptic rendering deteriorates at higher virtual wall stiffness values for all velocity estimation methods.

TABLE I

COMPARISON OF VARIOUS DIFFERENTIATION SCHEMES BASED ON K-WIDTH, B-WIDTH, MAXIMUM FIDELITY ERROR AND THE NUMBER OF TUNABLE PARAMETERS. THE NUMERICAL VALUES ARE OBTAINED EXPERIMENTALLY.

	FDM+filter	FOAW	AKF	Levant's differentiator
K-width (N/m)	$2.4 \times 10^4$	$2.1 \times 10^4$	$2.7 \times 10^4$	$3.6 \times 10^4$
B-width (Ns/m)	160	120	100	100
Tunable parameters	$\omega_c$	None	$q$	$\alpha, \lambda$
Max. fidelity error (Ns/m)	894.91	294.3	520.04	614.19

## VI. CONCLUSION

In this paper, we investigated the feasibility of Levant's differentiator for estimating velocity from position encoder data to increase the Z-width performance of haptic devices, and compared it with Finite difference method + lowpass filter, Kalman filter and First Order Adaptive Windowing velocity estimation schemes. We proposed a novel method for plotting Z-width, which combines the information about fidelity of the rendered haptic environment and practical device characteristics based on the frequency-response with the intuitive appeal of traditional Z-width obtained with the time-response of the haptic device. The proposed Z-width plotting method addresses the shortcomings of time-response based Z-width plot by capturing the practical device

limitations and also adding another dimension that informs about the accuracy of rendered virtual wall. Velocity estimation methods were evaluated using our proposed Z-width plotting scheme. Simulation and experimental results demonstrate that highest stiffness virtual walls were rendered using Levant's differentiator for velocity estimation, and FOAW was able to render virtual walls with highest fidelity. Insights gained through this study can be directly applied to surgical simulators that necessarily render complex virtual environments with high fidelity, and to haptic tele-manipulation of surgical robots that must faithfully and stably transmit a wide range of impedances.

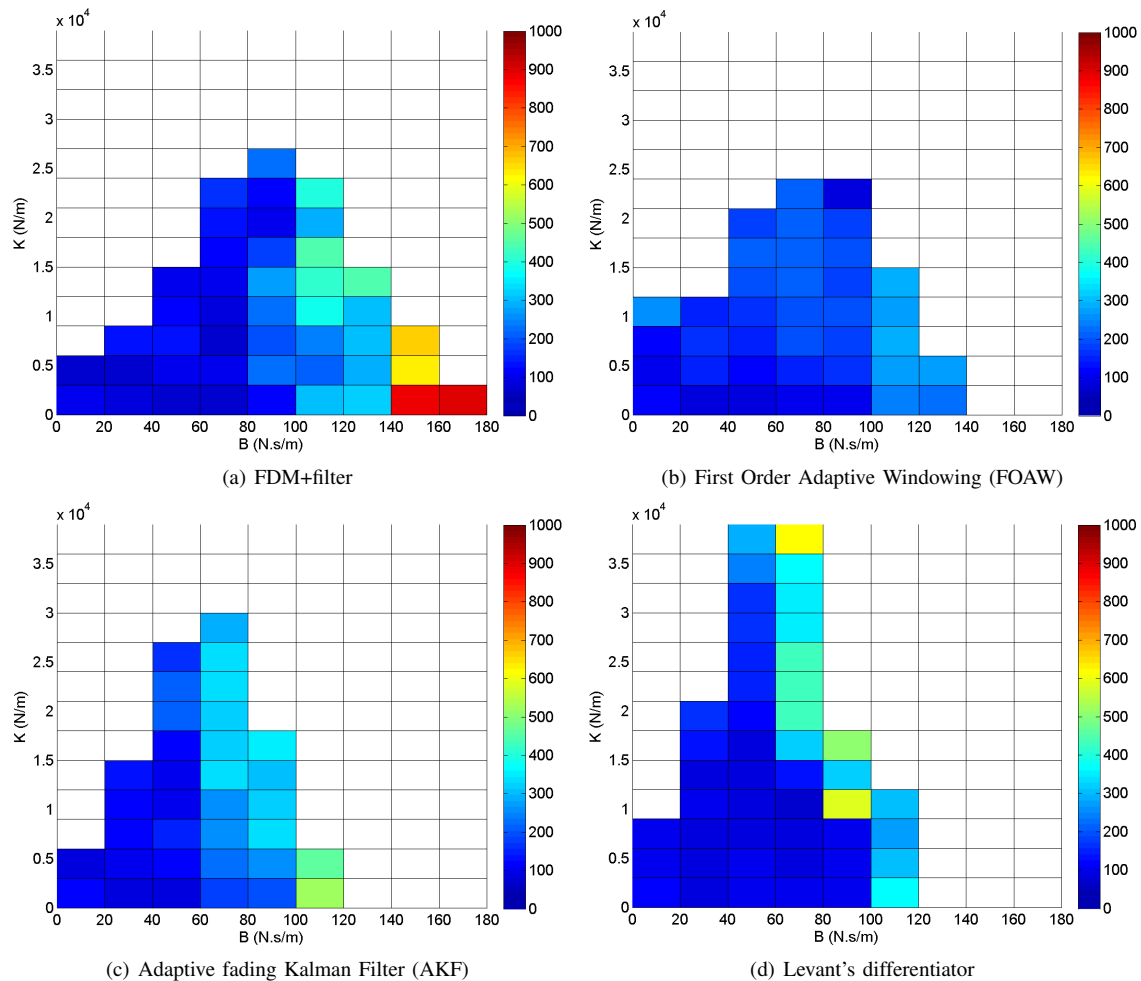


Fig. 8. Z-width plots obtained experimentally for various velocity estimation methods. The colorbar shows the RMS error (in N.s/m) between estimated and ideal virtual wall impedance. Similar observations as those in Fig. 7 can be made here.

#### ACKNOWLEDGMENT

This work was supported in part by the NSF Grant CNS-1136099.

#### REFERENCES

- [1] J. E. Colgate and J. M. Brown, "Factors affecting the z-width of a haptic display," in *IEEE International Conference on Robotics and Automation*, San Diego, CA, May 1994, pp. 3205–3210.
- [2] E. Samur, *Performance Metrics for Haptic Interfaces*. Springer Science & Business Media, 2012.
- [3] S. Abeywardena and C. Chen, "Implementation and evaluation of a three-legged six-degrees-of-freedom parallel mechanism as an impedance-type haptic device," *IEEE/ASME Transactions on Mechatronics*, 2017.
- [4] H. Bleuler, M. Bouri, L. Santos-Carreras, S. Gallo, A. Sengül, G. Rognini, and R. Clavel, "Trends in surgical robotics," *Romanian Journal of Technical Sciences*, vol. 58, no. 1-2, pp. 97–105, 2013.
- [5] M. K. O'Malley, K. S. Sevcik, and E. Kopp, "Improved haptic fidelity via reduced sampling period with an FPGA-based real-time hardware platform," *Journal of Computing And Information Science In Engineering*, vol. 9, no. 1, 2009.
- [6] J. S. Mehling, J. E. Colgate, and M. A. Peshkin, "Increasing the impedance range of a haptic display by adding electrical damping," in *IEEE World Haptics Conference*, March 2005, pp. 257–262.
- [7] D. Weir, J. Colgate, and M. Peshkin, "Measuring and increasing Z-width with active electrical damping," in *Symposium on Haptic Interfaces for Virtual Environments and Teleoperator Systems*. Reno, Nevada, USA: IEEE, March 2008, pp. 169–175.
- [8] O. Baser, H. Gurocak, and E. I. Konukseven, "Hybrid control algorithm to improve both stable impedance range and transparency in haptic devices," *Mechatronics*, vol. 23, no. 1, pp. 121–134, February 2013.
- [9] O. Baser, E. ilhan Konukseven, and H. Gurocak, "Stability and transparency improvement in haptic device employing both mr-brake and active actuator," in *21st IEEE International Symposium on Robot and Human Interactive Communication*. IEEE, 2012, pp. 12–18.
- [10] V. Hayward, F. Janabi-Sharifi, and C.-S. J. Chen, "Adaptive windowing discrete-time velocity estimation techniques: Application to haptic interfaces," in *Symposium on Robotic Control*, September 1997, pp. 465–472.
- [11] J. J. Gil, "Control de dispositivos fisicos de gran espacio de trabajo para la interaccion tactil con entornos virtuales," Ph.D. dissertation, Universidad de Navarra, 2003.
- [12] N. Colonnese and A. Okamura, "Stability and quantization-error analysis of haptic rendering of virtual stiffness and damping," *The International Journal of Robotics Research*, p. 0278364915596234, 2015.
- [13] V. Chawda, O. Celik, and M. K. O'Malley, "Application of Levant's differentiator for velocity estimation and increased Z-width in haptic interfaces," in *World Haptics Conference*. Istanbul, Turkey: IEEE, 2011, pp. 403–408.
- [14] P. R. Bélanger, P. Dobrovolny, A. Helmy, and X. Zhang, "Estimation of angular velocity and acceleration from shaft-encoder measurements," *The International Journal of Robotics Research*, vol. 17, no. 11, pp. 1225–1233, 1998.
- [15] V. Chawda, O. Celik, and M. K. O'Malley, "A method for selecting velocity filter cut-off frequency for maximizing impedance width performance in haptic interfaces," *Journal of Dynamic Systems, Measurement, and Control*, vol. 137, no. 2, p. 024503, 2015.
- [16] F. Janabi-Sharifi, V. Hayward, and C. S. J. Chen, "Discrete-time adaptive windowing for velocity estimation," *IEEE Transactions on Control Systems Technology*, vol. 8, no. 6, pp. 1003–1009, 2002.

[17] R. H. Brown and S. C. Schneider, "Velocity observations from discrete position encoders," in *Proc. SPIE 0858, Signal Acquisition and Processing, 1111*, November 1987.

[18] T. Ghaffari and J. Kovacs, "A high-performance velocity estimator for haptic applications," in *IEEE World Haptics Conference*, Daejeon, Korea, April 2013, pp. 127–132.

[19] R. H. Brown, S. C. Schneider, and M. G. Mulligan, "Analysis of algorithms for velocity estimation from discrete position versus time data," *IEEE Transactions on Industrial Electronics*, vol. 39, no. 1, pp. 11–19, 1992.

[20] A. Tilli and M. Montanari, "A low-noise estimator of angular speed and acceleration from shaft encoder measurements," *Automatika*, vol. 42, no. 3-4, pp. 169–176, 2001.

[21] M. Koul, M. Manivannan, and S. Saha, "Effect of dual-rate sampling on the stability of a haptic interface," *Journal of Intelligent & Robotic Systems*, pp. 1–13, 2017.

[22] S. Sinclair, M. M. Wanderley, and V. Hayward, "Velocity estimation algorithms for audio-haptic simulations involving stick-slip," *IEEE Transactions on Haptics*, vol. 7, no. 4, pp. 533–544, Oct 2014.

[23] P. Bhatti and B. Hannaford, "Single-chip velocity measurement system for incremental optical encoders," *IEEE Transactions on Control Systems Technology*, vol. 5, no. 6, pp. 654–661, November 1997.

[24] R. Merry, M. Van de Molengraft, and M. Steinbuch, "Velocity and acceleration estimation for optical incremental encoders," *Mechatronics*, vol. 20, no. 1, pp. 20–26, 2010.

[25] M. C. Cavusoglu, D. Feygin, and F. Tendick, "A critical study of the mechanical and electrical properties of the phantom haptic interface and improvements for high performance control," *Presence*, vol. 11, no. 6, pp. 555–568, December 2002.

[26] W. H. Zhu and T. Lamarche, "Damping enhancement of haptic devices by using velocities from accelerometers and encoders," in *Joint 48th IEEE Conference on Decision and Control and 28th Chinese Control Conference*, Shanghai, P.R. China, December 2009, pp. 7515–7520.

[27] Y. Aydin, O. Tokatli, V. Patoglu, and C. Basdogan, "Fractional order admittance control for physical human-robot interaction," in *World Haptics Conference (WHC)*. IEEE, 2017, pp. 257–262.

[28] O. Tokatli and V. Patoglu, "Stability of haptic systems with fractional order controllers," in *IEEE/RSJ International Conference on Intelligent Robots and Systems (IROS)*. IEEE, 2015, pp. 1172–1177.

[29] A. Levant, "Robust exact differentiation via sliding mode technique," *Automatica*, vol. 34, no. 3, pp. 379–384, 1998.

[30] J. Moreno and M. Osorio, "A Lyapunov approach to second-order sliding mode controllers and observers," in *IEEE Conference on Decision and Control*, Cancun, Mexico, December 2008, pp. 2856–2861.

[31] J. J. Gil and I. Díaz, "Method for estimating the stability boundary of impedance haptic systems," in *World Haptics Conference (WHC)*. IEEE, 2017, pp. 569–574.

[32] N. Colonnese, A. F. Siu, C. M. Abbott, and A. M. Okamura, "Rendered and characterized closed-loop accuracy of impedance-type haptic displays," *IEEE transactions on haptics*, vol. 8, no. 4, pp. 434–446, 2015.

[33] F. Janabi-Sharifi, V. Hayward, and C.-S. J. Chen, "Novel adaptive discrete-time velocity estimation techniques and control enhancement of haptic interfaces," *IEEE Trans. Control Systems Technology*, vol. 8, no. 6, pp. 1003–1009, 2000.

[34] A. Filippov and F. Arscott, *Differential Equations with Discontinuous Righthand Sides*. Springer, 1988.

[35] R. Pintelon and J. Schoukens, *System Identification: A Frequency Domain Approach*. John Wiley & Sons, 2004.

[36] A. Davila, J. Moreno, and L. Fridman, "Variable gains super-twisting algorithm: A lyapunov based design," in *American Control Conference*, Baltimore, MD, USA, July 2010, pp. 968–973.

[37] I. Salgado, I. Chairez, J. Moreno, and L. Fridman, "Design of mixed luenberger and sliding continuous mode observer using sampled output information," in *49th IEEE Conference on Decision and Control (CDC)*, Atlanta, Georgia, USA, December 2010, pp. 5138–5143.

[38] I. Salgado, J. Moreno, L. Fridman, A. Poznyak, and I. Chairez, "Design of variable gain super-twisting observer for nonlinear systems with sampled output," in *International Conference on Electrical Engineering Computing Science and Automatic Control*, Tuxtla Gutierrez, Mexico, September 2010, pp. 153–157.



**Vinay Chawda** received the B.Tech. and M.Tech. degrees in mechanical engineering from Indian Institute of Technology, Bombay, India in 2009, and his Ph.D. in mechanical engineering from Rice University, Houston, TX, USA in 2013. He was a Research Assistant at the Mechatronics and Haptics Interfaces (MAHI) Laboratory at Rice University from 2009 to 2013, and R&D Postdoctoral Associate at Disney Research from 2015 to 2016.

His research and development experience includes physical human-robot interaction, human interface devices, control of haptic interfaces and bilateral teleoperation systems. He was awarded the Best Paper Award at the 2011 IEEE World Haptics Conference in Istanbul, Turkey, and the Best Robotics Paper Award at the 2013 ASME Dynamic Systems and Controls Conference in Stanford University, CA, USA.



**Ozkan Celik** received the B.S. and M.S. degrees in mechanical engineering from Istanbul Technical University, Istanbul, Turkey, in 2004 and 2006, respectively. He received his Ph.D. degree in mechanical engineering from Rice University, Houston, TX, USA in 2011. He was a Research Assistant at the Mechatronics and Haptic Interfaces (MAHI) Laboratory at Rice University from 2006 to 2011. He served as an Assistant Professor of Mechanical Engineering at San Francisco State University (2011–2013) and at Colorado School of Mines (2013–

2017). He is currently a Servo Controls Engineer at the Mechatronics Center of Excellence within the Commons Solutions Group at Applied Materials, Inc. His research and development experience spans the fields of haptics, mechatronics, exoskeletons, rehabilitation robotics and predictive modeling and simulation.



**Marcia K. O'Malley** (SM13) received the B.S. degree in mechanical engineering from Purdue University, West Lafayette, IN, USA, in 1996, and the M.S. and Ph.D. degrees in mechanical engineering from Vanderbilt University, Nashville, TN, USA, in 1999 and 2001, respectively. She is currently the Stanley C. Moore Professor of mechanical engineering and of computer science and of electrical and computer engineering at Rice University, Houston, TX, USA, and directs the Mechatronics and Haptic Interfaces Laboratory. She is adjunct faculty in the

Departments of Physical Medicine and Rehabilitation at the Baylor College of Medicine and the University of Texas Medical School at Houston, and is the Director of Rehabilitation Engineering at TIRR-Memorial Hermann Hospital. Her research addresses issues that arise when humans physically interact with robotic systems, with a focus on training and rehabilitation in virtual environments. Prof. O'Malley is a Fellow of the American Society of Mechanical Engineers and serves as an Associate Editor for the ASME Journal of Mechanisms and Robotics, the ACM Transactions on Human Computer Interaction, and the IEEE Transactions on Robotics.